*Data and Metadata*. 2025; 4:765
doi: 10.56294/dm2025765

ORIGINAL

# A Lead-Acid Battery Discharge Emulator with a Hardware-in-the-Loop System for Low-Power General Applications

## Emulador de descarga de baterías de plomo-ácido con un sistema de hardware en el lazo para aplicaciones generales en baja potencia

Jhonny Barzola[1], Francisco Naranjo[1], Julio Guerra[1], Carlos Morán[1]

[1]Universidad Técnica del Norte (UTN), Facultad de ingeniería en ciencias aplicadas (FICA). Ibarra, Ecuador.

**Cite as**: Barzola J, Francisco Naranjo FN, Guerra J, Morán C. A Lead-Acid Battery Discharge Emulator with a Hardware-in-the-Loop System for Low-Power General Applications. Data and Metadata. 2025; 4:765. https://doi.org/10.56294/dm2025765

**Submitted:** 10-05-2024 **Revised:** 13-09-2024 **Accepted:** 29-03-2025 **Published:** 30-03-2025

**Editor:** Dr. Adrián Alejandro Vitón Castillo

**Corresponding Author:** Jhonny Barzola

**ABSTRACT**

This study addresses the critical need for efficient laboratory methods to test battery performance, identified through a bibliometric analysis of research trends in battery technologies, integration challenges, lifespan, and recovery. A key focus is the detailed evaluation of lead-acid batteries and battery emulators in electronic applications. The study highlights the significance of lead-acid battery discharge emulators as cost-effective and safe alternatives to actual batteries in laboratory testing, enabling controlled testing conditions. The system behavior was validated by employing a resistive load module and making comparisons with manufacturer data. Using this system and a resistive load module, its behavior was verified by comparing it with the data provided by the manufacturer. The next phase of this work involved selecting components to emulate the battery's behavior using a switched-mode power supply controlled by a current source and a mathematical model chosen from the Matlab-Simulink tool through a Hardware-in-the-loop (HIL) system that interprets the battery's state of charge (SoC) to match the pre-configured model response to the lead-acid battery manufacturer's data. The emulator circuit was thoroughly evaluated against the model's expected responses to various charge levels, culminating in the implementation of an integrated prototype that simulates the discharge of lead-acid batteries in low-power applications and introduces a user-friendly interface, facilitating its application in general engineering studies. The work offers a valuable tool for battery research and development, promoting advancements in the study of lead-acid battery discharge in low-power applications.

**Keywords:** Rechargeable Battery; Battery Emulator; Lead-Acid Battery; State of Charge; HIL System.

**RESUMEN**

Este estudio se centra en abordar la necesidad crítica de métodos eficientes para probar el rendimiento de las baterías en laboratorios, identificada a través de un análisis bibliométrico sobre la tendencia de investigación en baterías, sus tecnologías, los desafíos de integración, la vida útil y la recuperación, culminando en una exploración detallada de las baterías de plomo-ácido y los emuladores de baterías mediante aplicaciones electrónicas. Se destaca la importancia de los emuladores de descarga de baterías de plomo-ácido como herramientas alternativas a las baterías reales para las pruebas en laboratorio, debido a su capacidad para replicar condiciones de prueba controladas, mejorar la seguridad y reducir costos. Se desarrolló un sistema, seleccionando específicamente una batería de 12V 7Ah 20Hr con un sistema de monitoreo para el análisis. El comportamiento del sistema se validó mediante un módulo de carga resistiva y comparaciones con los datos del fabricante. Usando este sistema y un módulo de carga resistiva, se verificó su comportamiento comparándolo con los datos proporcionados por el fabricante. La siguiente fase de este trabajo consistió en seleccionar componentes para emular el comportamiento de la batería utilizando una fuente de alimentación conmutada controlada por una fuente de corriente y un modelo matemático elegido desde la herramienta Matlab-Simulink a través de un sistema Hardware-in-the-loop (HIL) que interpreta el estado de carga (SoC) de la batería para que la respuesta del modelo preconfigurado coincida con los datos del fabricante de la batería de plomo-ácido. El circuito emulador fue evaluado exhaustivamente en comparación con las respuestas esperadas del modelo a diferentes niveles de carga, culminando en la implementación de un prototipo integrado que simula la descarga de baterías de plomo-ácido en aplicaciones de bajo consumo y presenta una interfaz fácil de usar, facilitando su aplicación en estudios de ingeniería en general. El trabajo ofrece una herramienta valiosa para la investigación y el desarrollo de baterías, promoviendo avances en el estudio de la descarga de baterías de plomo-ácido en aplicaciones de bajo consumo.

**Palabras clave:** Batería Recargable; Emulador de Batería; Batería de Plomo-Ácido; Estado de Carga; Sistema HIL.

## INTRODUCTION

With the increasing adoption of renewable energy and electric vehicles, the study of batteries is crucial for their design, operation, and recycling.

Rechargeable electric batteries are widely used, from low-power portable devices to their growing integration in energy systems, electric vehicles, and small- to medium-scale energy storage. To evaluate the behavior of battery-dependent devices or assess the behavior of the batteries themselves, a set of batteries is required to be subjected to different levels of charge. Considering a large number of tests to be conducted, the use of real batteries is not practical. Rechargeable batteries are constantly evolving, as evidenced by a bibliometric study on the Scopus database, which analyzed 17 150 articles between 2011 and 2022, showing a co-occurrence rate of 18,52 % for the study of batteries on electric vehicles, followed by 6,98 % for energy storage, with 3311 publications in 2022 focused on electric vehicle development, compared to 446 publications in 2011, indicating a clear increasing trend.

A similar increasing trend is observed for lithium-ion batteries in electric vehicles, with a base of 5187 articles. The BATTERY 2030+ initiative, detailed in [3], focuses on the development of batteries in multidisciplinary emerging fields linked to traditional battery research. The initiative outlines a strategy with six fields, particularly emphasizing the use of new materials and intelligent parameter sensing, led by China and the United States in the last decade. It also highlights that studies mainly apply to battery electrolytes, but it is expected that the focus will also shift towards electrodes.

Battery operation is closely linked to optimization through machine learning algorithms, as indicated in a bibliometric study using a final selection of 17 high-impact articles from a filtered sample of 465 on battery and optimization topics. Sensing is an important part of battery operation study, referencing State of Charge (SoC), State of Health (SoH), and State of Power (SoP).

The use of batteries for mobility and storage, aiming to reduce pollution and gas emissions, is the subject of [5], focusing particularly on lithium-ion batteries. Another relevant topic is the reuse or recycling of battery parts. In a study [6] is presented a bibliometric study of technologies for metal recovery in lithium-ion batteries (LIBs), outlining a process that includes pre-treatment (discharge, disassembly, and segregation), metal extraction (pyro, hydro, or direct), and purification (precipitation, solvent extraction). Challenges in LIB recycling related to efficiency, cost, metal recovery (e.g., cobalt), and the constant development of new types of batteries are also discussed, with a recovery of only 20 % of the production cost limited by the recycling of just 5 % of used LIBs.

Electrode material and corrosion issues for batteries are also considered. A study on electrode corrosion in LIBs, lead-acid batteries, and, to a lesser extent, sodium, potassium, magnesium, and zinc-ion batteries is presented in [7]. The integration of electrolyte additives reduces water decomposition and electrode corrosion in lead-acid batteries, according to this study.

A review of battery technologies allows a comparison of properties obtained with the use of fuel cells, lead-acid batteries, or materials such as nickel, lead-acid, lithium-ion, zinc, sodium, and vanadium. Various properties are compared, such as nominal voltage, energy density, cycle life, charge and discharge efficiency, and cost. The review includes a comparison of lead-acid battery technologies: Flooded, Deep cycle, AGM, and Gel. It also covers a comparison of technologies for different types of LIBs and ultracapacitors. Additionally, in a research [8] are discussed the main causes of degradation in lead-acid batteries, including over-discharge, overcharge, sulfation, stratification, water loss, and short circuit.

A search in Scopus using the command “lead-acid OR lead acid OR pb AND batter*” yields 10 343 documents from the year 2000 to 2023 related to lead-acid batteries.

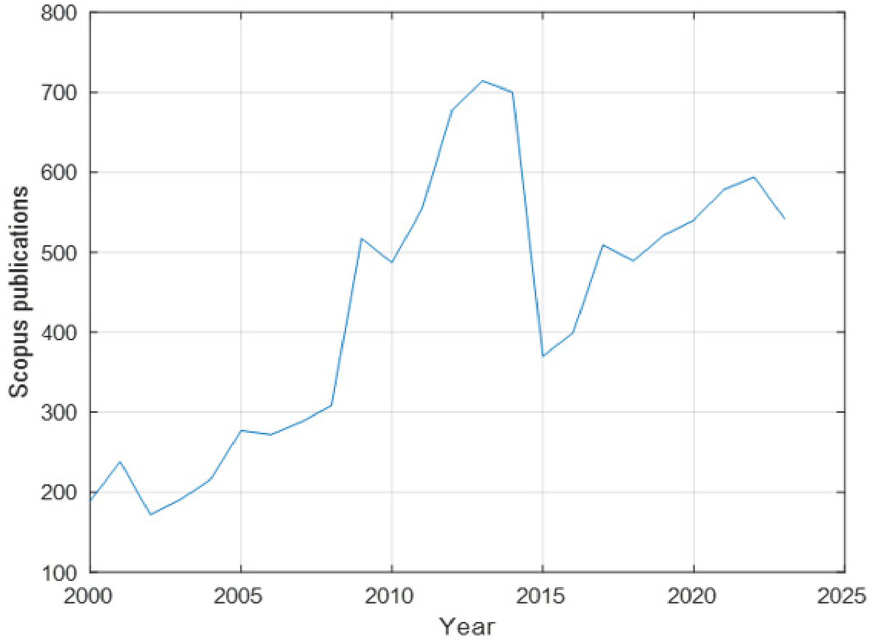


**Figure 1.** Publications about Lead-Acid batteries between 2000 and 2023

This graph shows that lead-acid batteries have seen increasing research interest, with a low point in 2015 of only 370 documents, as opposed to 714 documents in 2013. The leading countries in this research area are the United States and China.

A broader search using the command (lead AND batter*) between 2000 and 2023 yields 34 828 documents with a similar increasing trend and a low point in 2015 with 1412 documents, indicating a trend that could be the subject of further study.

Lead-acid batteries lead the market and maintain a strong position in the United States at 48 % compared to LIBs at 47 %, despite their limited number of cycles in heavy-duty charging applications and operation at low temperatures, which prevent their use as a power source in electric vehicles.[9] However, lead-acid batteries maintain a marketing advantage and an average of 80 % recycled components. Integration of carbon allotropes and metal oxides results in a considerable improvement in the performance of deep charge/discharge processes and reduces the irreversible sulfation phenomenon in conventional lead-acid batteries. Another successful strategy involves the integration of hybrid systems with supercapacitors.[10]

Even though lead-acid batteries are an old technology, they form the basis for the energy storage systems market. A study [11] provides a summary of aspects for the future development of lead-carbon batteries, outlining strategies for engineering, active materials or additives, interfaces, and cell design for a wide range of energy storage applications.

The use of real batteries for different research fields leads to excessive expenditure, risks of large discharges in uncontrolled environments, waiting time during battery recharging, and limited lifespan. In this regard, the use of emulators and approximate circuits controlled by algorithms becomes a solution for conducting operational tests and validating results. A study [12] examines the voltage, current, temperature, and interface constraints during the implementation of a battery cell emulator, as well as characterizing the hardware-in-the-loop (HIL) module using specific tools and a programming language interface.

The mathematical model used to emulate a battery must be selected according to the battery type. Hysteresis occurs between charge and discharge in lead-acid, nickel-cadmium, and nickel-metal-hydride batteries, regardless of the state of charge (SoC) of the battery, as detailed in [13] which includes experimental validation for electric vehicle applications. This study also provides an overview of mathematical models for the main battery types.

The ability to program the operation from a computer saves time between charging and discharging and allows the battery to be configured for different scenarios and charge levels. A study [14] showcases the implementation and evaluation of a scalable HIL battery prototype configurable for different battery types through programming commands.

There are also other important energy storage types for distributed generation development, general applications, and solutions to control and stability issues, as mentioned in [15]. This study also reviews relevant energy storage types—electrical, potential, and kinetic—to emphasize the future integration of energy using batteries as a control component and power contribution to the involved loads.

**Selection of mathematical model for the lead-acid battery**

The battery model developed in [13] serves as one of the foundational models implemented within the Simulink environment. Utilizing this model, it is possible to derive the charging behavior for lead-acid batteries as shown in equation 1:

$$V_{batt} = E_0 - Ri - k\frac{Q}{it-0.1Q}i^* - k\frac{Q}{Q-it}it + Exp(t) \quad (1)$$

Then, the battery discharge behavior can be mathematically represented as:

$$V_{batt} = E_0 - Ri - k\frac{Q}{Q-it}(it + i^*) + Exp(t) \quad (2)$$

Where:
$V_{batt}$=Battery voltage (V).
$E_0$=Battery constant voltage (V).
k=Polarization constant (V/Ah) or resistance (Ω).
Q=Battery capacity (Ah).
it=Actual battery charge (Ah).
Exp(t)=Exponential voltage zone (V).
R=Internal resistance (Ω).
i=Battery current (A).
i*=Filtered current (A).

These models are based on the simplest electrical circuit model for battery behavior, initially consisting of an ideal voltage source in series with an internal resistance, but this model does not consider the state of charge (SoC) of the battery. This is corrected with a model based on an open-circuit voltage in series with a resistance and RC circuits in parallel with an impedance. Through other modifications, the electrochemical behavior of a battery is also characterized, expressed in terms of terminal voltage, open-circuit voltage, internal resistance, discharge current, and state of charge. This equation, in addition to enabling the evaluation of the charging and discharging processes, provides an accurate representation of the battery's performance in various operating conditions.

Furthermore, this model was derived for discharge conditions but is also used for charging. It assumes constant internal resistance, capacity, and temperature during both charging and discharging, with the maximum capacity set to 100 % of the SoC. It also disregards self-discharge and battery memory. Manufacturers provide the battery's characteristic discharge curve in the datasheet, which can be used to calculate the voltage for a full charge as:

$$V_{full} = E_0 - Ri + A \quad (3)$$

Where:
$V_{full}$=Full charge voltage (V).
$E_0$=Battery constant voltage (V).
A=Exponential amplitude zone (V).

With these considerations, it is possible to calculate the end of the exponential region approximately after 3-time constants and the final nominal voltage region, where the voltage begins to drop abruptly. The latter is expressed as:

$$V_{nom} = E_0 - k\frac{Q}{Q-Q_{nom}}(Q_{nom} + i) - ri + AExp\left(-\frac{3}{QExp}Q_{nom}\right) \quad (4)$$

Where:
$V_{nom}$=Nominal voltage.
$Q_{nom}$=Nominal charge.

Finally, the time constant of the filtered current i* is determined experimentally. However, it is customary to use an approximate value of 30 seconds based on experience. For this study, a FirstPower FP1270 12V, 7Ah, 20Hr model battery with copper terminals was selected, which, according to its datasheet, has an internal resistance of 0,028 ohms and operates at 25 degrees Celsius with a range of 3 degrees Celsius. The full charge voltage is 13,8V, and the cutoff voltage is 9,6V for charges up to 60 % and 10,5V for lower charges, such as that registered for the 20-hour 5 % charge. These characteristics are illustrated in figure 2 through its characteristic graph for selected current levels. Other charge levels detailed in the manufacturer's datasheet regarding discharge time at different current levels can also be observed in this graph. This characteristic graph was obtained by modifying the parameters of the Simulink tool model.

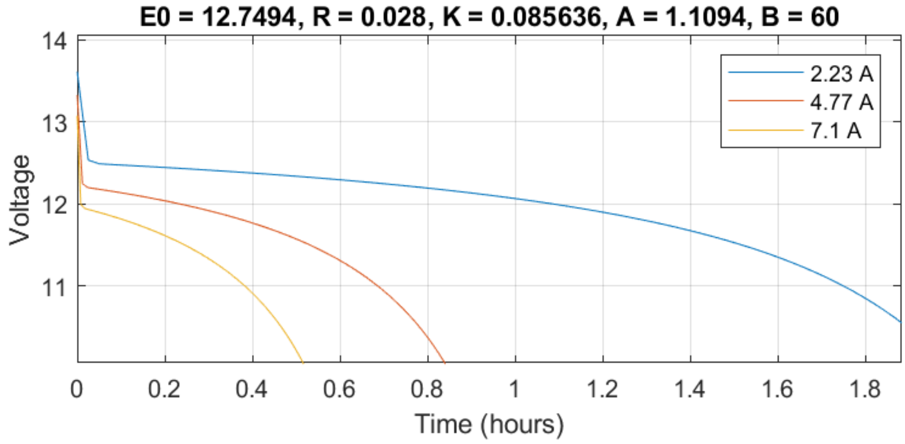


**Figure 2.** Voltage discharge at different load levels of the battery model

The selected current values correspond approximately to 31 %, 67 %, and 98 % of charge, which can be compared with the manufacturer's discharge profile in curves of approximately 0,3C, 0,6C, and 1C. It is also possible to evaluate the utilization zones and discharge times until the cutoff voltages.

Following this same principle, a study could be conducted for the charging profile of the lead-acid battery and the charging and discharging profile of other battery types. This work proposes emulating the discharged profile through an HIL system with the simulation model already studied for the FP1270 lead-acid battery and electronic components that enable emulation.

**Implementation of the hil system with the real battery**

Using the mathematical model as a tool, the behavior of a real battery was simulated, and parameters such as voltage, current, and state of charge (SOC) of a rechargeable electric battery were measured.

To verify the battery model, several simulations were conducted at different charge levels within a specific time interval of two hours, which were validated using an experimental circuit with the same charge values employed in the simulation based on the datasheet information. The loads selected were determined through an assessment of commercial resistors to maximize the power they could handle. For this purpose, the maximum battery values at 13,8V were chosen, along with small segments approaching the nominal 7-amp plate value. Segments of 20W were selected. This led to an estimated current value of 1,45 amperes to calculate the resistance value.

$$R_{Pmax} = \frac{V_{max}}{I_{max}} \qquad (5)$$

A value of 9,52 ohms is obtained for each charge segment. The commercial value selected consists of two 10W5R1J resistors in series for a total value of 10,2 ohms per segment. The total load will comprise 10 segments for a value of 1,02 ohms, where the 5 % tolerance of each resistor will not be considered in this study as no significant change in the desired results is expected with respect to the discharge curve of the emulator.

The aim of conducting simulation tests is to verify the operation of the selected battery model and validate its behavior under real conditions, like those of the lead-acid FP1270 battery. Table 1 lists the components used for the hardware-in-the-loop system, allowing constant monitoring of the battery's SoC, discharge current, and voltage.

To ensure a battery SoC of 100 % at the beginning of each test, an additional generic smart charger, specifically designed for motorcycle battery charging of the same size as the battery under study, was used. Figure 3 illustrates the setup of the components for monitoring the FP1270 battery. This involves using the analog inputs of the Arduino Mega2560 via signals from the ACS712 current sensors and the FZ0430 voltage sensor for the 10 switchable charge segments of the 10W5R1J resistors. The measurements are sent to the Matlab command platform for response evaluation and graph generation.

https://doi.org/10.56294/dm2025765

**Table 1.** Components of the HIL system for the FP1270 model battery and the loads module

| Component | Description |
|---|---|
| Battery | FP1270 |
| Development board | Arduino Mega 2560 |
| Voltage sensor | FZ0430 |
| Current sensor | ACS712 |
| Loads | 10W5R1J |

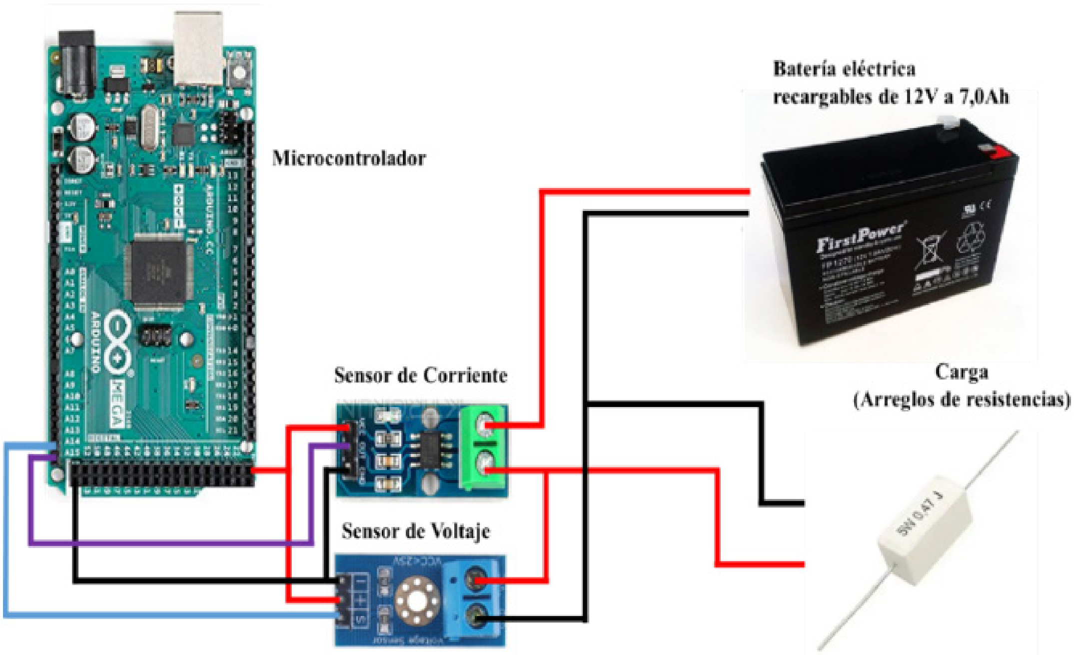


**Figure 3.** Diagram of the circuit for real battery discharge tests

With an initial 100 % SoC obtained from the battery with the help of the generic charger, voltage discharge curves are generated for a test at various charge levels based on the activated resistor segments for the evaluation of the actual battery using the proposed HIL system with the mentioned voltage and current sensors and interpreted through communication with a computer.

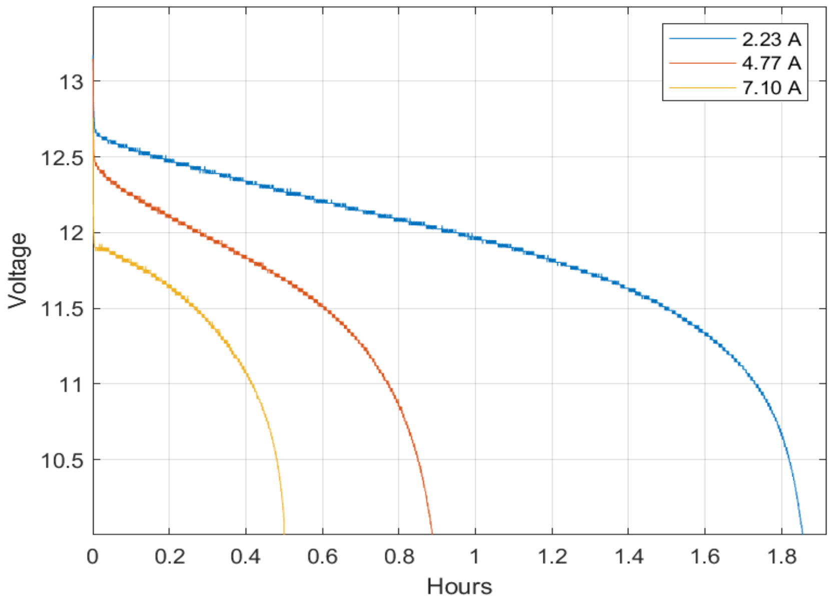


**Figure 4.** Voltage discharge curves at different load levels of the actual FP1270 battery

https://doi.org/10.56294/dm2025765

In figure 4, data for currents of 2,23; 4,77 and 7,10 amperes corresponding to 2, 4, and 6 resistor segments can be observed. Data acquisition was conducted at a frequency of one sample per second, resulting in a total of 3600 values per hour, aimed at collecting a significant amount of information that demonstrates the battery's behavior at different charge levels. Additionally, the current values labeled on each curve were taken after the exponential zone as an average of the values obtained in the utilization zone for a voltage drop with cutoff at 12 volts.

This result aligns with the information provided by the manufacturer regarding voltage discharge curves and with the discharge curves obtained in the Simulink tool. Similarly, the manufacturer provides a table of information regarding the discharge current profile, comparable to the figures obtained in this work. Through these tests, the simulation data and the operation of the HIL system for monitoring were also confirmed.

Another relevant aspect is the selection of the current levels in figure 2 for the model. These are comparable with those obtained in figure 4 in their real battery voltage response curves. Points of coincidence can also be observed regarding the discharge time up to the 10,5-volt cutoff, the discharge zone with a cutoff at 12 volts, and the exponential zone.

**Implementation of the experimental circuit of the discharge battery emulator**

To use the battery model validated in Simulink through an emulator, it is necessary to implement another experimental circuit that includes components to replace the battery. The other interface components should play the same role in acquiring voltage and current data when subjected to the same set of loads used with the actual battery. Table II shows the list of components selected for the battery emulator, highlighting the use of another measurement module for obtaining RMS values.

**Table 2.** Main elements of the battery circuit emulator

| Component | Description |
|---|---|
| Development board | Arduino Atmega2560 |
| Voltage and current sensor | PZEM 017 |
| Power source | Milenium Vip 24V/20ª |
| Converter | Full bridge converter IBT2 |
| Loads | 10W5R1J |

The mathematical model of the lead-acid battery to be used for emulation is interpreted through HIL communication of the electronic circuit with the Simulink tool. This option allows for data reading, recording, and subsequent analysis. In figure 5, the corresponding simulation can be observed to establish communication with the selected battery emulator electronic circuit.

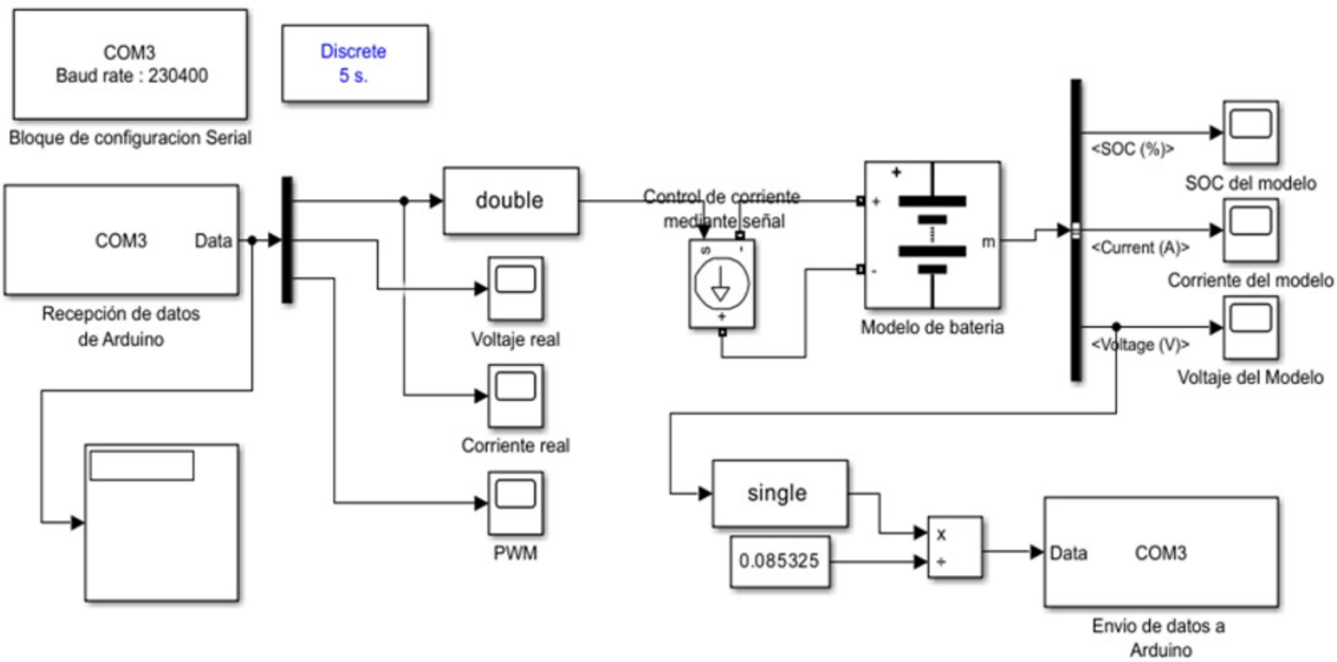


**Figure 5.** Block diagram of the Lead-Acid battery model with HIL integration

The power terminals of the full-bridge converter represent the emulated battery by switching the voltage of the power supply. These switches are controlled by the HIL system for the voltage and current signals from the PZEM 017 meter and interpreted by an RS485 module. This module has favorable characteristics for establishing HIL communication with the Simulink tool.

The power supply was oversized to the nominal charge current of the actual battery to enable emulating discharge curves at higher charge levels, as developed in the simulations and tests with the actual battery.

The command signals for the converter and the interpretation of the voltage and current signals are carried out through programming code in the microcontroller. Figure 6 shows the arrangement of the selected components for the electronic circuit, which also describes the operating methodology of the battery emulator.

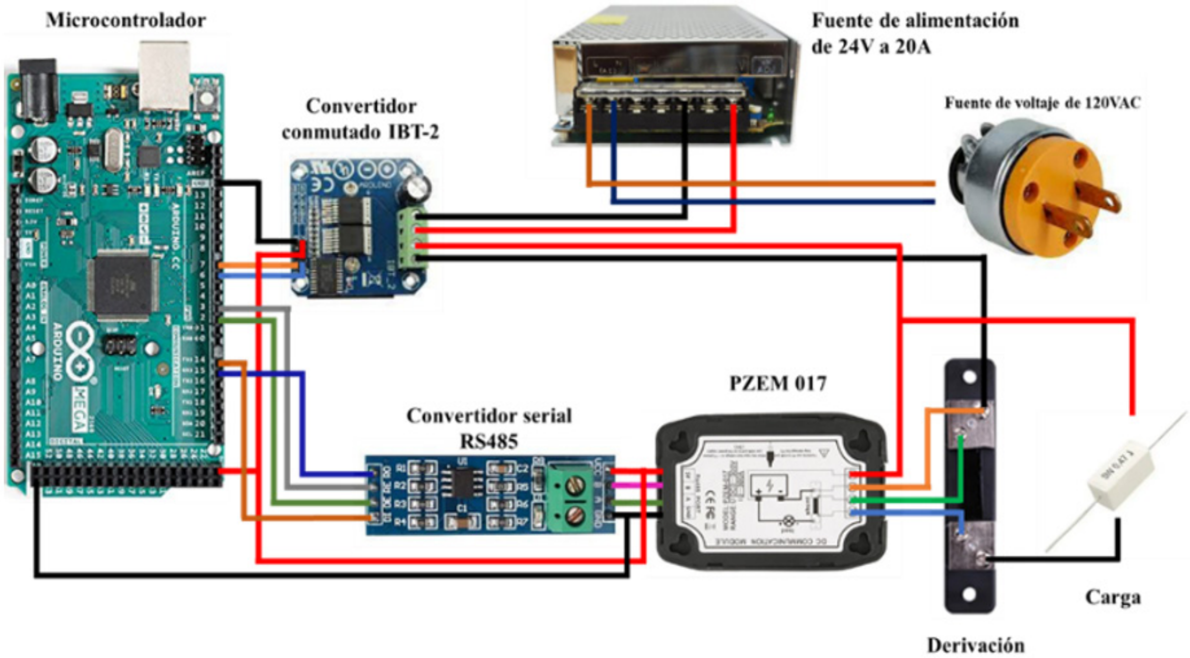


**Figure 6.** Battery emulator experimental circuit block diagram

The charge levels for two, four, and six load segments were selected in the mathematical model of the battery. These segments are equivalent to the current levels in which the actual battery was subjected, and with this arrangement, operational tests can be conducted at the same charge levels to which the actual battery was subjected, thereby evaluating the emulator's response.

**Functional tests of the emulator circuit and prototype construction**

The lead-acid battery emulator consists of five main components: the power supply, the full-bridge converter, the measurement system, the development board, and the Matlab interface with the Simulink tool for interpreting the mathematical model.

For the operation of the development board, a programming code was used to receive a voltage signal in PWM values and adapt them into digital outputs for the switched converter. Another stage of the code executes the acquisition of real voltage and current measurement data performed by the PZEM-017 and communication. The battery model interprets this data and uses it to simulate the behavior of a real battery for closed-loop operation.

This section is divided into two stages: discharge tests with the lead-acid battery emulator and the construction of a functional prototype containing both the actual battery used and the battery emulator circuit with the set of loads. This arrangement is the final goal of this work with the aim of having an emulator for future low-power battery discharge tests in general applications.

*Discharge tests of the emulator circuit*

The tests were conducted at the same load values corresponding to the two, four, and six segments as a reference, which in turn represent response curves of approximately 2,2, 4,7, and 6,9 amperes for a range of different load levels.

The tests were carried out by energizing the development board and circuit emulator components, initiating serial communication at 230 400 baud, and finally entering the load segments for measurements every 5 seconds. This time interval was selected based on experience in tests to reduce simulation times, which can take hours when using intervals shorter than five seconds, and to obtain good results with longer intervals exceeding 20 seconds. Figure 7 presents the result for two load segments, corresponding to an average current of 2,2 amperes.

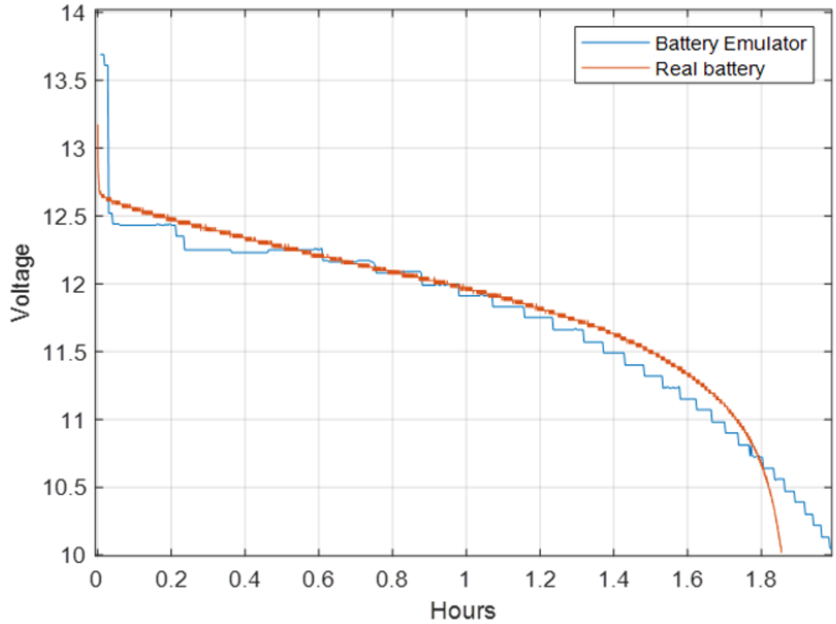


**Figure 7.** Voltage curve response of the emulator subjected to a load of 2,23A and compared with the voltage response of the real battery

The curve in blue observed in the figure 7 of the emulator circuit is quite to that has been obtained with the actual orange battery. An error can be observed in the initial exponential stage attributed to the initial response of the HIL system and emulator manipulation the first minutes. This, in turn, closely matches to the manufacturer's reference curve as previously verified at an approximate current level of 2,1 amperes or 0,3C, and also from the manufacturer's reference table regarding constant discharge currents at 25°C, from which some important values for this work are extracted in table 3.

**Table 3.** Constant discharge current reference values from the fp1270 battery manufacturer at 25°c

| Constant Current Discharge Characteristics (A, 25°C) | | | | | |
|---|---|---|---|---|---|
| F.V/time | 0,5h | 1h | 2h | 3h | 4h |
| 9,6V | 7,47 | 4,58 | 2,5 | 1,8 | 1,44 |
| 10,5V | 6,93 | 4,31 | 2,43 | 1,76 | 1,41 |

According to the manufacturer's data, at this constant temperature, an utilization time of one hour above 12 volts can be obtained for a load of 2,43 amperes, which can be verified with a very close curve for both the actual curve for an average load of 2,23 amperes for 3288 measurements, and for the emulator with an average current of 2,26 for 660 measurements. Furthermore, it is confirmed from the manufacturer a voltage cutoff of 10,5 volts after two hours, which for the actual battery and the emulator corresponds to just under 1,9 hours. This variation between the response curves of the actual battery and the manufacturer is mainly due to the lack of temperature control in the battery and the thermal effect not considered in the resistive loads, which was not so relevant initially, given that the main objective was to achieve a curve similar to that of the actual battery with the emulator. The emulator, on the other hand, is less affected by the temperature in the cutoff zone. However, the results are valid for the emulation of the studied battery in relation to the operating time in the utilization zones up to just before the cutoff voltage, which corresponds to what is used for general application tests.

Likewise, in figure 8, the response of the actual battery compared to that of the emulator for an average load of 4,77 amperes can be observed. In this case, a minute scale was selected considering the expected discharge time as a response.

In the manufacturer's reference case, it can be observed that for a constant load of 4,2 amperes or the representative 0,6C of 60 % of load, the region of utilization over 12 volts for 30 minutes is obtained, and a cutoff voltage of 10,5 volts is reached at 60 minutes of operation. Similarly, it shows with the data from Table III that for a constant discharge of 60 minutes at 4,31 amperes, a cutoff voltage of 10,5 volts is reached, and with 4,58 amperes, 9,6 volts is reached. For the 4,77 amperes load of the experiment, the utilization time of 20 minutes above 12 volts can be observed for both the actual battery and the emulator, with a cutoff voltage at approximately 53 minutes. The results obtained reflect an appropriate behavior of the actual orange curve of the actual battery and the blue curve of the emulator, considering that the experiment uses a slightly higher discharge current than that seen in the manufacturer's reference.

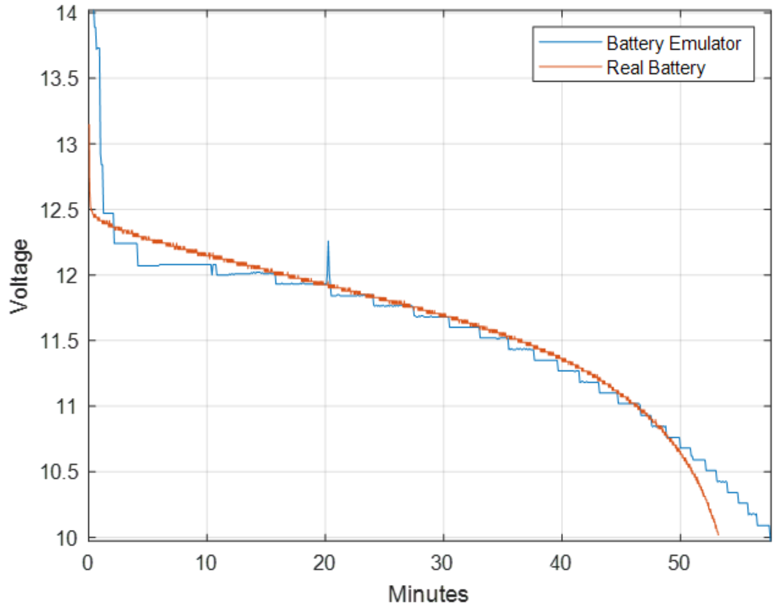


**Figure 8.** Voltage curve response of the emulator subjected to a load of 4,77A and compared with the voltage response of the real battery

Another result considered in the experiment is the outcome at a current level similar to that of a 7Ah battery. In figure 9, the result at 7,1 amperes of load can be seen, which closely corresponds to the information provided by the manufacturer in the 1C curve and the constant current discharge table at 6,93 amperes seen in Table III. The information mentions that a voltage of 10,5 volts is obtained after 30 minutes, a result that is comparable to the actual orange curve of the real battery, and with an even better response for the emulator compared to the manufacturer's data.

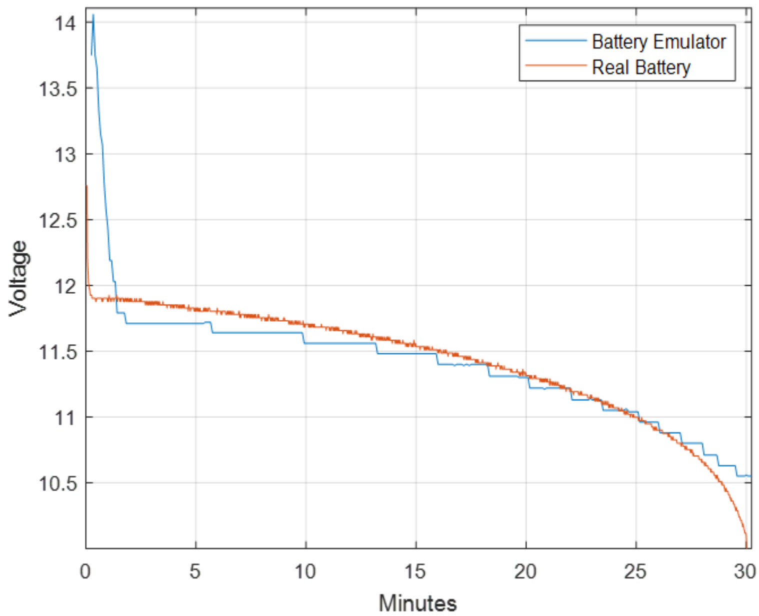


**Figure 9.** Voltage curve response of the emulator subjected to a load of 7,10A and compared with the voltage response of the real battery

Once the emulator circuit has been evaluated in terms of its response to different load levels and HIL interface to meet the selected mathematical model, a final stage is required where all the components are integrated into a robust functional prototype.

It is worth emphasizing that this study focuses on the "real" output voltage response of the power converter to the loads for different load currents, as it is a characteristic parameter of the actual battery. However, through the mathematical model in the Simulink tool, measurements of current response, battery state of charge (SoC), and the same on the output side of the model going to the converter control stage for voltage and current can also be obtained. This is achieved through a measurement file from which measurements can be extracted for further study.

*Implementation of the battery emulator prototype*

The proposed battery emulator prototype in this work consists of three main parts. The first part is the actual FP1270 battery alongside the generic charger, which enables charging and discharging to obtain voltage and current discharge graphs from the actual battery through the initially proposed HIL system connected to the development board. A drive switch and a three-position selector for charging or discharging action are added to the charger.

The second part is the array of resistive loads used for the tests with the 10 established sections to allow a suitable range of load capacity and performance tests. This module enables real battery discharge tests and the use of loads in the battery emulator prototype to visualize voltage and current discharge curves. The resistive load module simulates the load that the battery would typically receive in a real electrical system, allowing evaluation of the emulator prototype's behavior and obtaining results comparable to real situations through a series of switches and connection terminals for the equivalent resistance.

The third part consists of the emulator circuit with a main switch and connection terminals. The circuit emulator module is the main part of this project, as it is responsible for emulating the behavior of an electrical battery with an HIL monitoring system.

The circuit comprises a 6-amp main circuit breaker, from which a branch is taken for the power supply with internal fuse protection. The power supply output terminals are connected to the input terminals of the switched converter in its power stage. The outputs of the switched converter are connected to the terminals of the PZEM-017 and its branch, allowing voltage and current measurements. The power terminals of the PZEM-017 are connected to the battery emulator output terminals, which correspond to the power outputs of the converter. These emulator outputs, through terminals, allow connection to the resistance module or different external loads.

As mentioned earlier, the battery charger output is connected to the first position of a three-position rotary switch. In this switch position, the charger enables battery charging, the second position allows battery disconnection, and the third position enables the battery outputs for conducting real battery discharge tests.

Once the distribution of the electrical parts of the prototype was established, a design with the layout of all the components was defined. The aesthetic disposition of the elements making up the emulator prototype was selected for the front part of the design. The upper part was designated for the resistance module outputs, with the 10 switches and a general output in two female terminals marked as positive and negative, respectively.


**Figure 10.** Front view of the prototype battery emulator module

https://doi.org/10.56294/dm2025765

In the middle and to the left, the emulator circuit outputs are located, with two female terminals also marked with positive and negative, respectively, and a switch that directly activates the power supply.

In the middle and to the right, the outputs of the actual battery are situated with connection terminals for the loads and a branch in the three-position switch to allow its charging through the generic charger, which includes a display screen.

At the bottom, there is a space with a USB connection output for the Arduino Mega 2560 development board, enabling data acquisition using the MATLAB-Simulink interface via a computer. Additionally, the battery charger screen for manual configuration, if necessary, is in the bottom right.

The proposed prototype design features an intuitive layout, leading to the implementation shown in figure 10. The selector's position indicates the intended function: charging the actual battery in the "Charge" position, discharging the actual battery in the "Discharge" position, or operating the emulator circuit in the "Disconnect" position. The terminals are labeled with red for positive terminals (letter "P") and black for negative terminals (letter "N") to assist the user in connecting the load module to the emulator circuit or the actual battery.

At the rear of the prototype, only the main circuit breaker and a 110VAC power cable input required for the entire system are located. In figure 11, the internal layout of the prototype can be observed with all the previously mentioned components for the different functions of this prototype.

**Figure 11.** Internal distribution of the components in the emulator prototype

The connections of all the elements were made in a way that ensures they do not present any issues during handling or transportation of the module. As seen in figure 11, the integration of a PCB with connection terminals and auxiliary connection cables with terminals at all connection points for all the components of the prototype can be observed. For the power circuit connections, a 14 AWG conductor was used, and for control circuits, a 22 AWG conductor. Terminals were soldered to the conductors to prevent disconnection during handling, and heat-shrink tubing was used to ensure there are no short circuits or contacts between different elements.

All connections were made using different intuitive colors for different functions with the aim of establishing an intuitive pattern. Furthermore, a user manual was drafted with the programming codes for the development board to manipulate the different functions and the possibility of modifications through future work, as well as for the maintenance of the prototype if necessary.

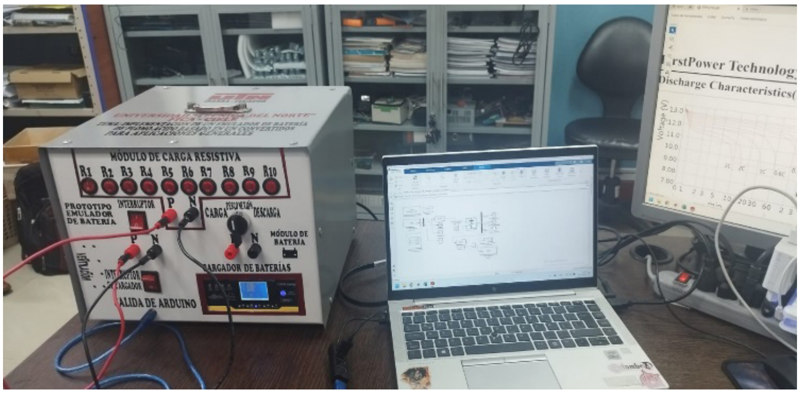


**Figure 12.** Discharge operation test with the encapsulated emulator prototype and its components

https://doi.org/10.56294/dm2025765

For handling the prototype and conducting general performance tests, only male connection cables from the actual battery or the emulator to the load module are required. The other physical components result from the selector function position and the operation of the battery charger power switch or the emulator circuit power switch, and the operation of the different load switches.

In figure 12, the emulator prototype is observed during validation tests with all its integrated components, connection cables to the emulator, the selector in the disconnect position, and the established communication through the USB cable with the MATLAB-Simulink HIL interface to interpret the mathematical model during discharge via a computer.

To conduct different operating tests on a real battery, it is necessary to ensure that the battery is fully charged before starting the discharge tests. This ensures obtaining a curve closer to the expected one under ideal conditions. The battery charging time depends on the previous discharge it has undergone in tests; the battery charger switch is activated, and the selector is placed in the battery charging position. The charger automatically detects the charge level and initiates the charging process automatically. This activity clearly indicates a significant time waste between tests mentioned among the issues of not having a battery emulator circuit like the one developed in this work to restart tests at 100 % SoC of the battery. Similarly, the advantage in terms of the lifespan of the emulator circuit compared to the real battery, even under the best usage conditions, and the lesser impact of temperature on its operation, as already observed in the resulting curves at higher currents, become evident.

As mentioned earlier, the dynamic current response and state of charge (SoC) can also be considered with the emulator for the case study. For this purpose, a dynamic discharge test was carried out with the emulator prototype to outline the dynamic voltage, current, and SoC response profile to the selected load variations in the experiment.

The figure 13 shows an example of the current emulator response for different randomly selected load levels for a three-segment drive for an average current of 3,25 amperes up to 8 minutes, then an increased load for 6 segments for a current of 6,48 amperes up to 15 minutes, where a release was made to four load segments corresponding to an average current of 4,5 amperes up to 23 minutes of battery emulation. Finally, two transitions were made corresponding to a reduction of two load segments for a current of 2,38 amperes up to completing 31 minutes, followed by an increase in load of 5 segments in the simulation resulting in an average current of 5,2 amperes for a waveform with a steeper slope up to 50 minutes, at which point the test was decided to be terminated due to the discharge level that the emulated battery would already have fallen below 10 volts below the breakdown voltage.

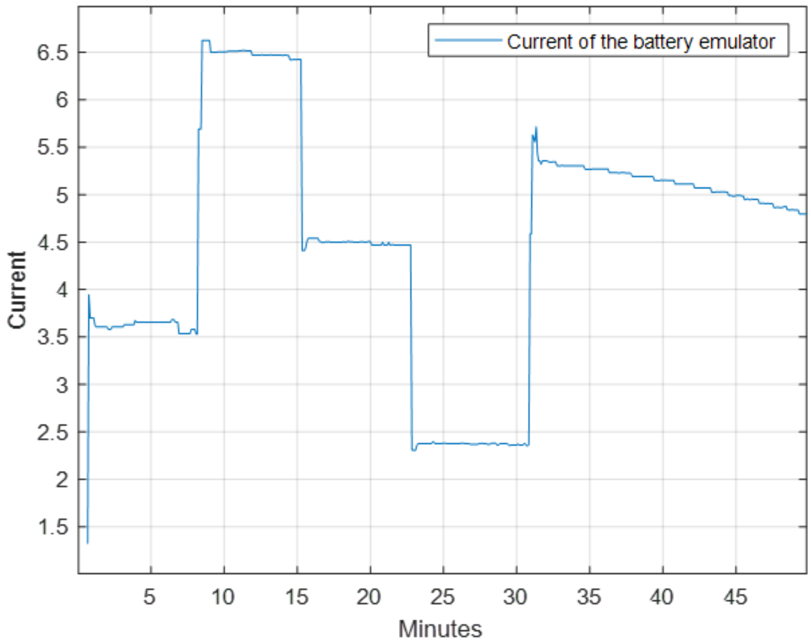


**Figure 13.** Dynamic discharge current response curve of the battery emulator

Similarly, we can observe in figure 14 the dynamic state of charge (SoC) response profile of the battery emulator to the selected load variations for the same experiment that produced the current response in figure 13, which has already been analyzed. The slope pattern of the response can be observed during the different transitions carried out during the experiment.

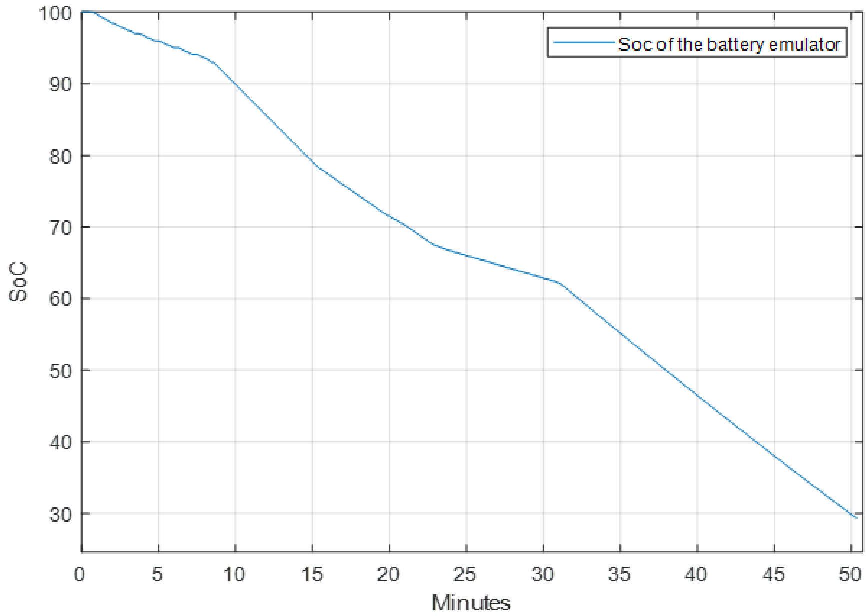


**Figure 14.** Dynamic State of Charge (SoC) profile of the battery emulator

Finally, figure 15 shows the voltage response of the experiment conducted for different load segment levels. This graph can be analyzed based on the times at which the respective transitions and load current changes were made. The transitions were highlighted while explaining figure 13, corresponding to 8, 15, 23, and 31 minutes, respectively. It can also be observed that from the 34th minute of emulation, the model's response curve begins to enter the knee point voltage for a rapid discharge, leading to the experiment's termination at 50 minutes below the 10-volt threshold. The 10,5-volt cutoff voltage was undercut after 45 minutes of emulating the battery.

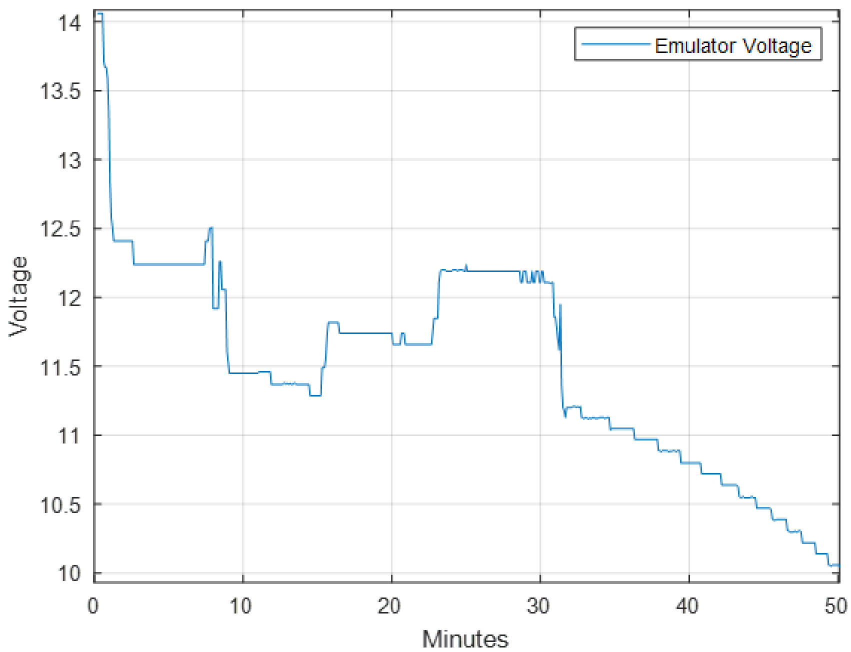


**Figure 15.** Dynamic voltage profile of the battery emulator

The implementation of this prototype constitutes a low-cost basis for reducing the use of test batteries in laboratories when the focus is on obtaining the appropriate response profile to emulate the discharge behavior of a real battery rather than the transient response profile. It is also important to emphasize the need for implementing temperature control in the HIL system for the emulator and real battery. Another necessary aspect is the use of temperature-controlled loads and the evaluation of the prototype with other types of batteries with a lower recycling rate, such as lithium-ion batteries, which have seen significant growth in the battery market due to their application in electric mobility. Finally, the prototype presented in this work offers a low-cost alternative for emulating the behavior and monitoring during battery discharge testing in the laboratory.

## CONCLUSIONS

The research trend regarding batteries is increasing according to the bibliometric study conducted in this work. Lead-acid batteries are the future basis for battery studies in terms of their market space and reuse system through recycled parts compared to other types of batteries. The importance of a battery state monitoring system in emulation systems was also confirmed through a review of previous works.

A battery emulator prototype with a hardware-in-the-loop system was presented in this work for general low-power applications, through the evaluation and emulation of a 12-volt, 7-ampere, 20-hour lead-acid battery. The emulator circuit has the capacity to monitor voltage, current, state of charge (SoC) output from a selected mathematical model, as well as the measured signals in the power stage subjected to loads with favorable results of a maximum difference of 0,2V between the real battery and the HIL emulator with the same current load, in order to neglecting the variability induced by the temperature. The emulator circuit offers multiple advantages over real batteries, such as lifespan, a variety of battery models or types, charging times or start at 100 % SoC, natural discharge, model corrections for temperature effects, equipment costs, connection and disconnection times, interface for real-time measurement visualization, and many other applications in laboratory settings where the evaluation of battery-dependent equipment and the assessment of different types of batteries are required. The emulator circuit was developed using generic components for a wide, cost-effective component disposition, allowing for future work planning related to improving the model's response to temperature variations and the inclusion of other types of battery for study.

## BIBLIOGRAPHIC REFERENCES

1. I. Ullah, M. Safdar, J. Zheng, A. Severino, and A. Jamal, "Employing Bibliometric Analysis to Identify the Current State of the Art and Future Prospects of Electric Vehicles," Energies, vol. 16, no. 5, 2023, doi: 10.3390/en16052344.

2. S. Chen, J. Xiong, Y. Qiu, Y. Zhao, and S. Chen, "A bibliometric analysis of lithium-ion batteries in electric vehicles," Journal of Energy Storage, vol. 63, 2023, doi: 10.1016/j.est.2023.107109.

3. P. Ahlgren, T. Jeppsson, E. Stenberg, E. Berg, and K. Edström, "BATTERY 2030+ and its Research Roadmap: A Bibliometric Analysis," ChemSusChem, vol. 16, no. 21, 2023, doi: 10.1002/cssc.202300333.

4. N. Hananda et al., "Battery optimization by machine learning algorithms: Research gap via bibliometric analysis," in E3S Web of Conferences, 2023. doi: 10.1051/e3sconf/202338801020.

5. Y. Ren et al., "A Comprehensive Review of Key Technologies for Enhancing the Reliability of Lithium-Ion Power Batteries," Energies, vol. 16, no. 17, 2023, doi: 10.3390/en16176144.

6. R. Rautela, B. R. Yadav, and S. Kumar, "A review on technologies for recovery of metals from waste lithium-ion batteries," Journal of Power Sources, vol. 580, 2023, doi: 10.1016/j.jpowsour.2023.233428.

7. P. Du et al., "Research progress towards the corrosion and protection of electrodes in energy-storage batteries," Energy Storage Materials, vol. 57, pp. 371–399, 2023, doi: 10.1016/j.ensm.2023.02.028.

8. A. Townsend and R. Gouws, "A Comparative Review of Lead-Acid, Lithium-Ion and Ultra-Capacitor Technologies and Their Degradation Mechanisms," Energies, vol. 15, no. 13, 2022, doi: 10.3390/en15134930.

9. K. Yanamandra, D. Pinisetty, and N. Gupta, "Impact of carbon additives on lead-acid battery electrodes: A review," Renewable and Sustainable Energy Reviews, vol. 173, 2023, doi: 10.1016/j.rser.2022.113078.

10. N. Vangapally et al., "Lead-acid batteries and lead–carbon hybrid systems: A review," Journal of Power Sources, vol. 579, 2023, doi: 10.1016/j.jpowsour.2023.233312.

11. J. Yin et al., "Lead-Carbon Batteries toward Future Energy Storage: From Mechanism and Materials to Applications," Electrochemical Energy Reviews, vol. 5, no. 3, 2022, doi: 10.1007/s41918-022-00134-w.

12. A. Verani, R. di Rienzo, N. Nicodemo, F. Baronti, R. Roncella, and R. Saletti, "Modular Battery Emulator for Development and Functional Testing of Battery Management Systems: Hardware Design and Characterization," Electronics (Switzerland), vol. 12, no. 5, 2023, doi: 10.3390/electronics12051232.

13. O. Tremblay and L.-A. Dessaint, "Experimental validation of a battery dynamic model for EV applications," in 24th International Battery, Hybrid and Fuel Cell Electric Vehicle Symposium and Exhibition 2009, EVS 24, 2009, pp. 930–939.

14. B. Halivni, D. Beniaminson, L. Maman, A. Yankovich, M. Evzelman, and M. M. Peretz, "Scalable High-Power Battery Emulator for Power Hardware-in-the-Loop Applications," in 2023 IEEE 24th Workshop on Control and Modeling for Power Electronics, COMPEL 2023, 2023. doi: 10.1109/COMPEL52896.2023.10221018.

15. J. Barzola, D. L. Simonetti, and J. F. Fardin, "Energy storage systems for power oscillation damping in distributed generation based on wind turbines with PMSG," in CHILECON 2015 - 2015 IEEE Chilean Conference on Electrical, Electronics Engineering, Information and Communication Technologies, Proceedings of IEEE Chilecon 2015, 2016, pp. 655–660. doi: 10.1109/Chilecon.2015.7404640.

## FINANCING
The authors did not receive financing for the development of this research.

## CONFLICT OF INTEREST
The authors declare that there is no conflict of interest.

## AUTHORSHIP CONTRIBUTION
*Conceptualization:* Jhonny Barzola.
*Data curation:* Jhonny Barzola.
*Formal analysis:* Francisco Naranjo.
*Research:* Carlos Moran.
*Methodology:* Francisco Naranjo.
*Project management:* Julio Guerra.
*Resources:* Julio Guerra.
*Software:* Carlos Morán.
*Supervision:* Jhonny Barzola.
*Validation:* Jhonny Barzola.
*Display:* Francisco Naranjo.
*Drafting - original draft:* Carlos Morán.
*Writing - proofreading and editing:* Jhonny Barzola.